https://doi.org/10.5194/wes-2024-24
Preprint. Discussion started: 29 April 2024

eawe european academy of wind energy
Open Access WIND ENERGY SCIENCE DISCUSSIONS

Dynamic Modelling and Response of a Power Cable connected to a Floating Wind Turbine

David Robert Verelst[1], Rasmus Sode Lund[1], and Jean-Philippe Roques[2]

[1]Frederiksborgvej 399, Building 118, DK-4000, Roskilde, Denmark
[2]TotalEnergies – One Tech, 92078, Paris La Défense, France

Correspondence: David Robert Verelst (dave@dtu.dk)

Abstract.

A power cable that connects a floating power plant to the grid is exposed to a dynamic environment that can pose challenging design conditions for the cable. This dynamic environment is caused by the movements of the floating substructure due to a combination of wind, wave and current forces. The power cable model needs to be able to account for its bending and axial stiffness, and hydrodynamic forcing. In this publication a catenary mooring/cable line element with bending stiffness is verified with a reference tool to assure the bending stiffness of a power cable is captured correctly. By using an existing parametric design model, a simple power cable design (in terms of overall cable length) is proposed for the IEA15MW turbine with UMaine floating substructure for a site with a water depth of 82 meter. A simple geometric method is proposed to initialize this complex lazy wave cable design in a dynamic and time domain simulation environment. The hydro-servo-aero-elastic wind turbine simulation environment HAWC2 is then used to establish an estimate of how much movements the combined system (turbine, floater, mooring lines, and power cable) experiences. This study discusses the necessary steps that are to be considered when including the dynamic power cable in the analysis and when adjusting a floating reference wind turbine design to a specific site with different water depth.

1 Introduction

In this study a proof-of-concept is presented that discusses some of the analysis steps that are necessary to consider a site suitability assessment study of an existing floating wind turbine reference design and extend that with a dynamic power cable. The steps that are discussed in more detail here are:

- the modelling of the dynamic power cable (section 3)
- the design of the lazy wave shape and cable properties (sections 4.2, 4.1
- initialisation strategy in a dynamic simulations environment such as HAWC2 (section 4.3
- adjustment of mooring lines to a new water depth (section 5.1
- platform motion initial screening based in simple set of load cases (section 5.3

https://doi.org/10.5194/wes-2024-24
Preprint. Discussion started: 29 April 2024

eawe european academy of wind energy
Open Access WIND ENERGY SCIENCE DISCUSSIONS

– platform motions under a broader but still reduced set of operating conditions (section 5.4

This study is concluded with additional remarks on what other steps and iterations are needed before concluding on the suitability of a reference design with dynamic power cable to a new site.

2 HAWC2 simulation complex

The work in this study is performed using the hydro-aeroe-servo-elastic framework HAWC2 Larsen a Hansen (2023) and relies on several of the available sub-modules such as ESYSMooring Hansen and Kallesøe (2011) to simulate mooring lines and ESYSWamit Hansen (2014) to capture the hydrodynamic response of the floater. ESYS refers to the External System interface that is available in HAWC2 and that allows users to develop sub-modules that are tightly coupled into the HAWC2 solver. In this context the tight coupling refers to directly injecting additional elements into the constrained equations of motion, and which are then solved by HAWC2. HAWC2 is a multi-body framework that contains various aerodynamic engineering models focused around calculating the forces on horizontal axis turbines. The modelling approached for this study is the traditional Blade Element Momentum (BEM) code and is further extended with a range of corrections (dynamic inflow, grid-based induction, dynamic stall, etc) Madsen et al. (2020). Further, a linear Timoshenko beam element (see Kim et al. (2013); Pavese et al. (2015)) can account for the structural flexibility. When combined with a sufficient number of bodies in the floating frame of reference the non-linear geometrical response is captured accurately Gözcü and Verelst (2020).

3 Cable element with bending stiffness

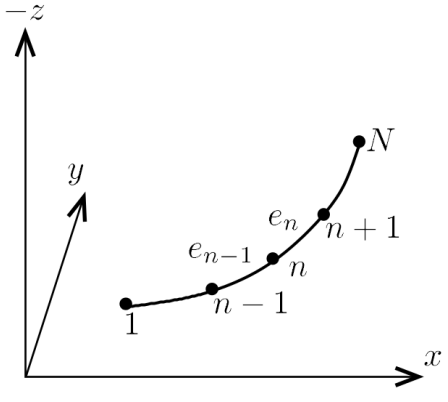

Figure 1. Elements of a single mooring line segment in ESYSMooring

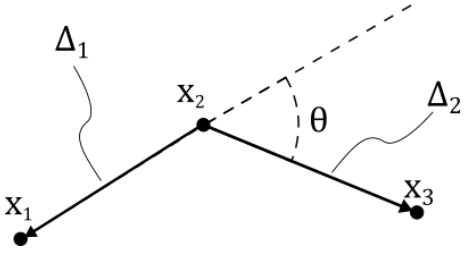

Figure 2. Bending stiffness is applied between three nodes and is a function of the given angle θ

The dynamic power cable is modeled as a traditional catenary mooring line element in ESYSMooring (and is based on Bergan et al. (1985)) for which now also bending stiffness is added. In ESYSMooring each line segment has constant structural

https://doi.org/10.5194/wes-2024-24
Preprint. Discussion started: 29 April 2024

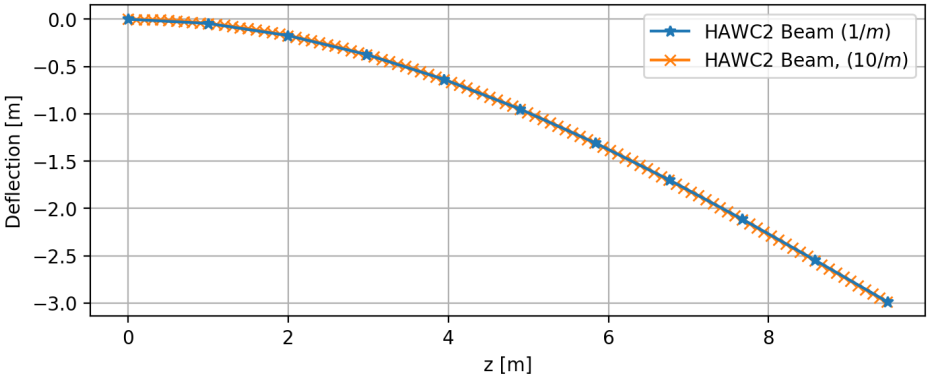

Figure 3. Verification that the chosen beam discretization of 1 structural element per meter is sufficiently converged.

and hydrodynamical properties, and each element along the line segment is considered linear (see figure 1). Each node is constrained to the next via a ball joined constraint. The restoring bending moment between two elements of the dynamic cable is then proportional to the angle θ in figure 2 and its defined bending stiffness.

Beam	EI bending stiffness $[Nm^2]$	EA axial Stiffness $[Nm^2]$	mass $[kg]$
Bernoulli-Euler	$2 \cdot 10^6$	-	0
HAWC2 Beam	$2 \cdot 10^6$	$2 \cdot 10^{10}$	0
ESYSMooring	$2 \cdot 10^6$	$2 \cdot 10^{10}$	0

Table 1. Beam properties used for the verification cases shown in figure 3 and 4. Note that the same axial and bending stiffness is used as for the lazy wave cable in table 2

The cable element with bending stiffness is verified against two different models: the HAWC2 Timoshenko beam element and the cable element from the commercial software package DeepLines. For the comparison with the HAWC2 Timoshenko beam element a cantilever beam subject to a constant load at the tip is used. The verification between HAWC2 ESYSMooring and DeepLines uses the same lazy wave cable shape as presented in section 4.2.

In HAWC2 a relevant Timoshenko beam problem is set up such that the amount of curvature obtained is similar to what is observed in the lazy wave cable shape. By using the same stiffness properties as the reference cable sufficient curvature (meaning similar to the maximum curvature of the lazy wave shape) is obtained by applying a $m = 2{,}000\text{kg}$ lumped tip mass. In figure 3 the authors first confirm a chosen discretion of 1 structural beam element per meter is sufficient by comparing it with a solution that contains 10 elements per meter.

In figure 4 the deflection curves are compared between an analytical Bernoulli-Euler solution, the HAWC2 Timoshenko beam, and the ESYSMooring implementation outlined in this publication (see section 3). Note that the properties of the beam are summarized in table 1. Further, three different discretizations for the ESYSMooring element are shown: 1,2 and 4 elements per meter. The results show a good agreement between the models considering the following observations:

https://doi.org/10.5194/wes-2024-24
Preprint. Discussion started: 29 April 2024

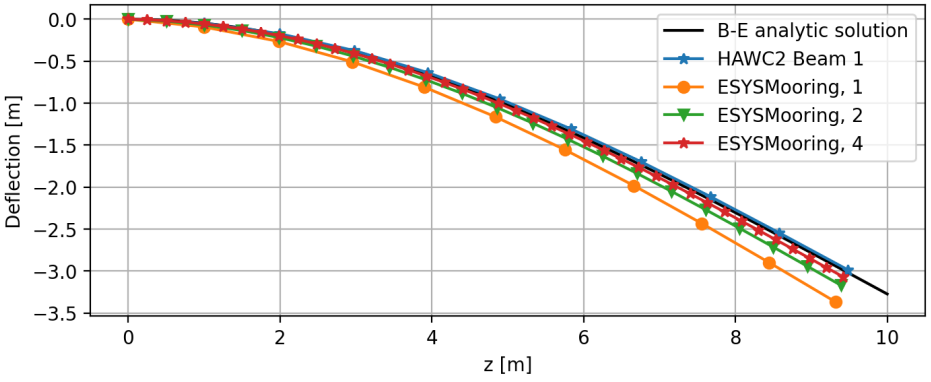

Figure 4. Comparison of a 10m beam deflected by a 2,000kg tip mass using 3 different models, and 3 different descretizations for the ESYSMooring model.

- The analytical model shows very good agreement with the HAWC2 Timoshenko model, except that the former does not account for the non-linear geometrical response (the beam essentially becomes longer).
- ESYSMooring provides the best match with HAWC2 Timoshenko when using a 4 times more elements (1 per meter compared to 4).
- For the remainder of this publication a descretization of 1 element per meter for ESYSMooring is chosen to strike a balance between computational effort and accuracy.

As the last step in the verification process of the ESYSMooring model a lazy wave cable shape (see figure 5 is compared with results obtained from the software package DeepLines. The comparison considers the cable node positions (see figure 5), the bending moment distribution (see figure 6) and the effective tension (see figure 7) in the cable. With the effective tension it is assumed that the internal cable pressure equals the external pressure in the water, and that the hydrostatic pressure does not affect the tension/pressure in the cable. A good agreement between HAWC2 ESYSMooring and DeepLines is observed. This verification example and the corresponding HAWC2 input files can be found in Lund and Verelst (2024).

4 Lazy wave design and modelling in HAWC2

Note that the HAWC2 input files needed to reproduce this study (including the verification cases) can be found in Lund and Verelst (2024).

4.1 Dynamic power cable properties

Obtaining representative specifications of a state-of-the-art dynamic power cable is within an open academic context not straight forward since cable providers consider this information as confidential. In Rentschler et al. (2019) structural cable

https://doi.org/10.5194/wes-2024-24
Preprint. Discussion started: 29 April 2024

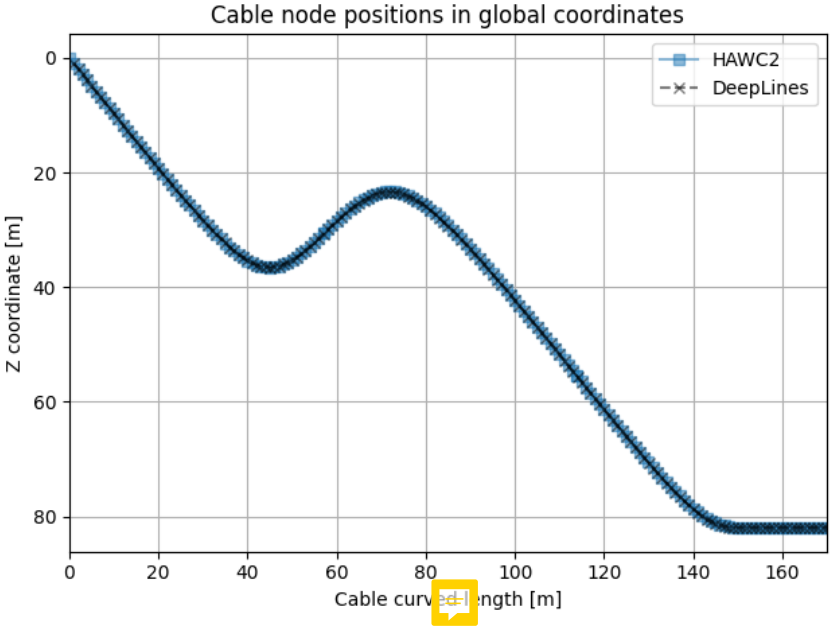

Figure 5. Comparison between the nodal positions of the model in HAWC2 ESYSMooring and DeepLines for the dynamic cable in a static lazy wave condition.

properties are used that have been reported earlier by Thies et al. (2012) and date back a decade relative the current publication. Further, Rentschler et al. (2019) states that the lack of access to representative structural properties of the cable is limiting the scope of publicly accessible research efforts.

The cable properties used for this study are listed in table 2. Note that the lazy wave cable concept has increased buoyancy in the mid section. For this publication it as assumed that the buoyancy section does not affect the stiffness properties.

	cable	cable + buoyancy element
Outer radius [mm]	200	~~306~~ 423
Nominal weight in air [N/m]	706	1129
Nominal weight in seawater [N/m]	390	-316
Bending stiffness EI [kNm^2]	10	10
Axial stiffness EA [MN]	700	700

Table 2. Dynamic cable properties used for the lazy wave, taken from Rentschler et al. (2019); Thies et al. (2012). Note the reference seems to contain an inconstancy since the reported 306 mm outer radius of the buoyancy section can not float the combined cable and buoyancy elements. By considering an outer diameter of 423 mm this is rectified, and a similar lazy wave shape as reported by the reference is obtained.

https://doi.org/10.5194/wes-2024-24
Preprint. Discussion started: 29 April 2024

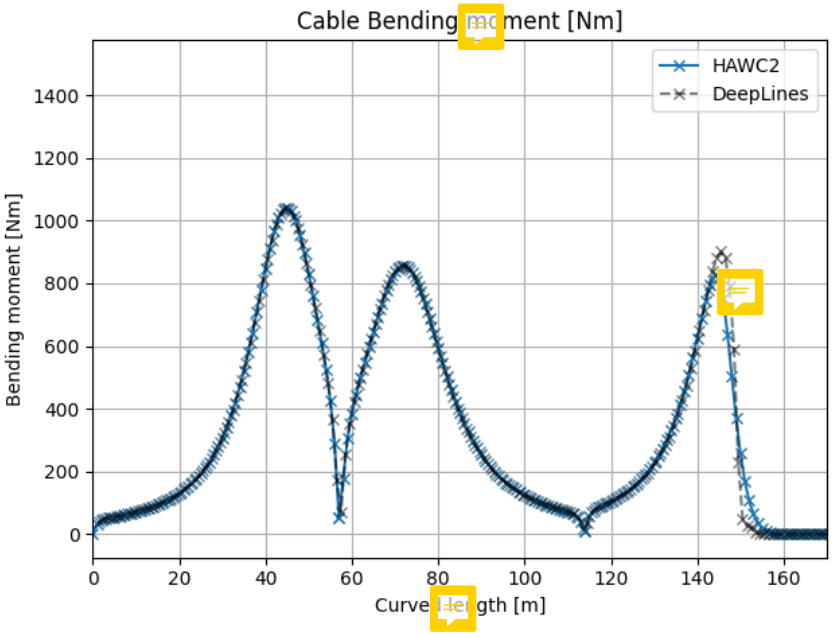

Figure 6. Comparison between the bending moment of the model in HAWC2 ESYSMooring and DeepLines for the dynamic cable in a static lazy wave condition.

4.2 Sizing the lazy wave

The lazy wave cable shape used for this publication is based on a parametric design model described by Rentschler et al. (2019) and is illustrated in figure 8. In Rentschler et al. (2019), a first design iteration of the lazy wave is suggested by evaluating the fitness of the cable considering the maximum allowable curvature (MAC) and minimum breaking load (MBL) of the cable (see expression 1). By considering a range of water depths h (see figure 8), the shortest cable configuration out of the best (as defined by equation 1) 10 solutions is chosen for each respective depth, and length fractions for the three different parts of the cable configuration are reported and included here in table 3. For the lazy wave discussed here the values are simply scaled according to the relevant water depth of $h = 82\mathrm{m}$.

$$\text{fitness} = \frac{\rho_{max}}{MAC} + \frac{T_{max}}{MBL} \tag{1}$$

Note that an important simplification regarding lazy wave cable configuration used for this publication and Rentschler et al. (2019) is that bend-stiffener is excluded from the analysis. Instead, the cable is connected to the platform via a hinge connection or ball bearing joined (fixed in translation, free in rotation).

https://doi.org/10.5194/wes-2024-24
Preprint. Discussion started: 29 April 2024

eawe european academy of wind energy
Open Access WIND ENERGY SCIENCE DISCUSSIONS

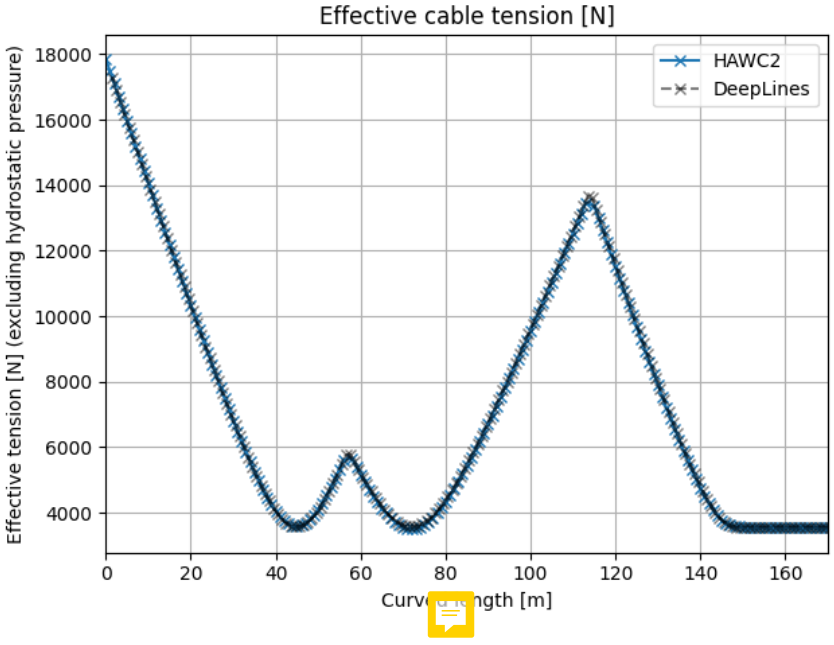

Figure 7. Comparison between the effective tension of the model in HAWC2 ESYSMooring and DeepLines for the dynamic cable in a static lazy wave condition.

	$h = 70$m	$h = 82$m	$h = 100$m
	Rentschler et al. (2019)	this publication	Rentschler et al. (2019)
l_{total}/h	2.74	2.76	2.79
l_1/l_{total}	0.25	0.25	0.24
l_2/l_{total}	0.25	0.25	0.24
l_3/l_{total}	0.47	0.50	0.49

Table 3. Parametric configuration of the lazy wave selected for this publication in combination with values reported for similar water depths in Rentschler et al. (2019).

4.3 Model initialisation in HAWC2

In general a HAWC2 ESYSMooring simulation starts at $t = 0$ from either a straight line (by defining the coordinates that indicate the start and the end of the line), or a full list of coordinates for each node on the line. In this case, the objective is to
95 determine a simple geometric description of all nodes that is fast to derive and from which the HAWC2 simulation is able to arrive at a converged hydrostatic solution in a time domain simulation. To this end, the initial lazy wave shape is defined as three connected (partial) circles (see figure 8). To solve this geometrical problem, the following conditions should be met:

https://doi.org/10.5194/wes-2024-24
Preprint. Discussion started: 29 April 2024

eawe european academy of wind energy
Open Access WIND ENERGY SCIENCE DISCUSSIONS

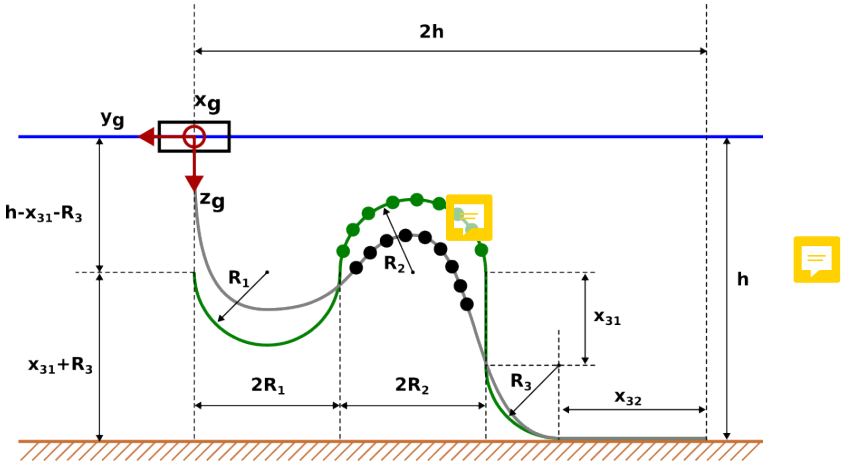

Figure 8. Parametric description of the lazy wave cable design (black) and the simplified geometric initialisation shape used in HAWC2 (green). The circles in the model indicate the second cable segment has a positive buoyancy.

$$h \geq R_2 + R_3 + x_{31} \tag{2}$$

$$l_3 = x_{31} + x_{32} + R_3\pi/2 \tag{3}$$

By combining 2 and 3 we get:

$$x_{32} \geq h - R_2 + (\pi/2 - 1)R_3 - l_3 \tag{4}$$

A solution can be established by simply choosing a value for $x_{32} \geq 0$ and $R_3 \geq 5$ (considering the circle consist of straight elements with a length of 1m, a value larger than 5 is practical).

In order to practically divide a circle segment into a discrete number of nodal positions and assure the integrated length (following straight lines between the nodes, not an analytical arc) is exactly as intended, the algorithm starts with specifying the number of elements needed to cover the cable length and then find numerically the corresponding radius that is required to exactly match a piece-wise linear circle satisfying the length constrained. Note that all the Python implementation details and source code can be found in Lund and Verelst (2024).

Note that as part of the initialisation process in HAWC2, the starting point of the cable will be moved at constant speed from its initial position (which is located $h - x_{31} - R_3$ below the actual connection point, as can be seen in figure 8) to the final connection point at the floater. By performing a long enough initialisation run a steady state lazy wave cable shape is obtained (in which a balance is reached between inertial and buoyancy forces) and saved, and from which subsequent simulations can start. This shape is also used for the comparison between HAWC2 ESYSMooring and DeepLines as outlined in section 3.

https://doi.org/10.5194/wes-2024-24
Preprint. Discussion started: 29 April 2024

eawe european academy of wind energy
Open Access WIND ENERGY SCIENCE DISCUSSIONS

5 Preliminary analysis of a site specific IEA15MW and UMaine semi-sub case study

5.1 Turbine, floater and mooring line model

As practical example to illustrate the functionality/capability of the cable element with bending stiffness a case study of a floating offshore wind turbine system is conducted. The model consists of the IEA 15 MW offshore reference turbine Gaertner et al. (2020), and the UMaine VolturnUS-S semi-submersible reference floating platform Allen et al. (2020). The platform is secured to the seabed using a three line mooring system, with equiangular catenary lines spaced 120° apart. For this study the water depth was changed from the 200m (as used by Allen et al. (2020)) to an undisclosed site with a 82m water depth. The mooring line configuration was scaled such that the same catenary shape was maintained for this more shallow site. The updated mooring line lenght is 821m long, and extends radially 853m from the center of the platform. Note that this is only slightly shorter than the original 850m mooring line length as for the 200m water depth site. For the more shallow site a relatively longer part of the mooring line that was resting over the ocean floor was needed to avoid the platform displacements lifting the mooring line up entirely and loading the anchor directly when considering the initial screening of the platform motions described in section 5.3.

The mooring lines are modelled in ESYSMooring using a classical catenary element without bending stiffness (see also section 3). The hydrodynamic modelling of the mooring lines and dynamic cable include buoyancy and drag forces (using a classical Morrison approach). The dynamic power cable is connected to the floating platform from below in the center, and is locked in the three translational degrees of freedom but excludes a bend-stiffener. Note that there are two power cables: one coming in from a neighbouring turbine, and one going out towards the next turbine in the array (or a collection station if it is the first turbine in the array). For this analysis both cables are assumed to be aligned (so shifted with 180 degrees). The power cable and the mooring system is illustrated in figure 10. The structural response of the power cable is modelled including bending stiffness as described in section 3.

With the new mooring line configuration an updated response decay test was executed to verify the natural periods of the combined floater and mooring line system was still close to the original design. A small but acceptable difference in periods was observed (see table 4).

	Floater period [s]		
	82m	200m	pct difference
surge	139	142	2.1%
sway	139	142	2.1%
heave	20.4	20.4	0.0%
pitch	28.9	27.7	-4.3%
roll	28.9	27.7	-4.3%

Table 4. Comparison of the combined mooring-floater-turbine response to a decay tests for the original 200m water depth configuration and the adjusted 82m for this publication.

https://doi.org/10.5194/wes-2024-24
Preprint. Discussion started: 29 April 2024

eawe european academy of wind energy
Open Access WIND ENERGY SCIENCE DISCUSSIONS

5.2 Reduced set of site specific load cases

For the analysis presented here the wind, wave and current conditions are taken from a confidential measurement campaign at and undisclosed but relevant site. Further, a reduced set of load cases is considered of "only" 162 extreme cases (see table 5) and 2250 normal operational cases (see table 6). A full site suitability assessment for a floating wind turbine would otherwise (considering both extreme and life time fatigue) consists of 100,000 cases (order of magnitude). The HAWC2 input files for these simulation cases can be found in Lund and Verelst (2024).

5.3 Initial screening of floating platform response

An initial investigation of the effect of the dynamic cable on the overall response of the platform is conducted. The purpose of this investigation is to explore whether the angle at which the cable is connected to the turbine, β in figure 10, has a significant effect on the overall turbine response. Further, this analysis establishes a first iteration of the platform motion envelope. The conditions under which this reduced analysis is performed is outlined in table 5. The simulations include variations in the wind direction and angle of the cable connection. Wind and wave direction is the same but the water current is not included yet in this first screening.

Parameters	N	**Values**
Wind speed	1	12 m/s
Wind direction	9	[0°, 15°, 30°, 45°, 60°, 75°, 90°, 105°, 120°]
Cable connnection angle	6	[15°, 30°, 45°, 60°, 75°, 90°]
Waves	1	$H_s = 12.50$m, $T_p = 18.40$s
Wave direction	1	Same as wind direction
Current	1	0 m/s
Turbelence seeds	3	[-]
Total	162	

Table 5. Set of environmental simulation conditions to determine the first screening of the floater displacement envelope as function wind, wave, mooring line and dynamic cable configuration angle. The column N indicates how many independent realizations are considered of each variable. The wave parameters are obtained from a measurement campaign and depict the omnidirectional wave parameters with a return period of 50 years.

An illustration of the mean platform position in the cartesian plane is shown in figure 9. The results of the simulations show that, as expected, the the mean floater position is dependent on the wind and wave direction. It further shows that the angle of the dynamic cable does not contribute to the mean positional response of the platform. This is also to be expected since the lazy wave shape is designed such that the cable is not expected to carry any of the station keeping loads of the platform.

https://doi.org/10.5194/wes-2024-24
Preprint. Discussion started: 29 April 2024

eawe european academy of wind energy
Open Access WIND ENERGY SCIENCE DISCUSSIONS

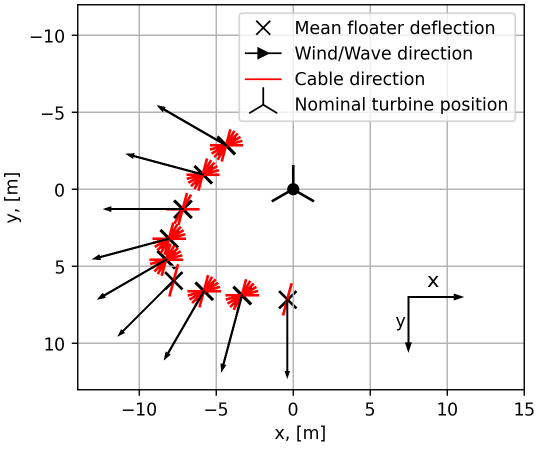

Figure 9. Floater displacements according to conditions defined in table 5. Note the cable orientation (red lines) do not affect the mean displacements.

5.4 Floating platform response under normal operating conditions

A more comprehensive set of conditions is considered for a second screening round of the floater response. Three different wind speeds are considered in this reduced set of normal operating conditions: $8\mathrm{m/s}$, $12\mathrm{m/s}$ and $16\mathrm{m/s}$. This corresponds to one wind speed below-, one around-, and one above rated. The current is assumed independent of the wind speed, and current speeds of $0.15\mathrm{m/s}$ and $0.25\mathrm{m/s}$ are considered and are based on the available measurement data.

Due to the shape of the floater (the angular repetition), the span of the wind and current directions can be reduced to $120°$. The resolution of the wind and current directions are limited to 5 points each: $(0°, 30°, 60°, 90°, 120°)$. A wind/wave misalignment with a span of $\pm 40°$ is considered, resolved in 5 points. The significant wave height H_s, and the corresponding period for the waves T_p are calculated from the wind speed according to (5) and (6).

$$H_s = 0.4 \cdot \bar{\mathrm{U}} \tag{5}$$

$$T_p = 1.33 + 4.74\sqrt{H_s} \tag{6}$$

The turbulence intensity, TI is calculated according to (7)

$$\mathrm{TI} = \frac{\left(\mathrm{TI}_{ref}\left(0.75\bar{\mathrm{U}} + 5.6\right)\right)}{\bar{\mathrm{U}}} \tag{7}$$

For each realization of the set of variables, simulations with 3 turbulence seeds are considered. The total number of simulations, and the contribution of each of the variables is shown in table 6.

All the directional quantities are defined according to figure 10, positive clockwise. The 0-angle of waves and current is aligned with the 0-angle of the wind in HAWC2.

https://doi.org/10.5194/wes-2024-24
Preprint. Discussion started: 29 April 2024

WIND ENERGY SCIENCE DISCUSSIONS

Parameters	N	Values
Wind speed	3	[8 m/s, 12 m/s, 16 m/s]
Wind direction	5	[0°, 30°, 60°, 90°, 120°]
Waves	1	$H_s = 0.4$Wind Speed, $T_p = 1.33 + 4.74\sqrt{H_s}$
Wave direction	5	Wind direction + [-40°, -20°, 0°, 20 °, 40 °]
Current	2	[0.15 m/s , 0.25 m/s]
Current direction	5	[0°, 30°, 60°, 90°, 120°]
Turbulence seeds	3	[-]
Total	2250	

Table 6. Contribution of each of the variables to the total number of combinations in the set. the column N indicates how many independent realizations are considered of each variable. The wave parameters are obtained from a measurement campaign and for which a normal sea state (NSS) statistical model was derived.

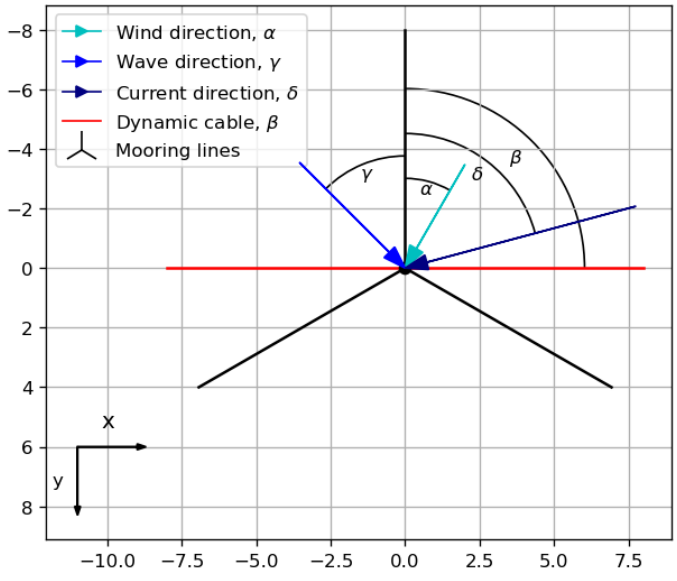

Figure 10. Illustration of how the wind-, wave- and current direction are defined in the simulation setup. The HAWC2 coordinate system is drawn in the lower left-hand corner. Note that the y-axis has been inverted.

Focusing again on the floater response, a selection of the results of the operational load cases defined in table 6 are shown in figure 11 in which the mean and standard deviation of the floater are given (σ and μ respectively). To put the displacements into context, also the platform size and shape is included in the figure. A closer look on the cases with a wind direction of 0°is given in figure 12. Here also the wave and current direction are indicated. What can be noticed from both figure 11 and 12 is that the main driver of the platform position is the wind, and to a lesser extend the waves and current. When compared

https://doi.org/10.5194/wes-2024-24
Preprint. Discussion started: 29 April 2024

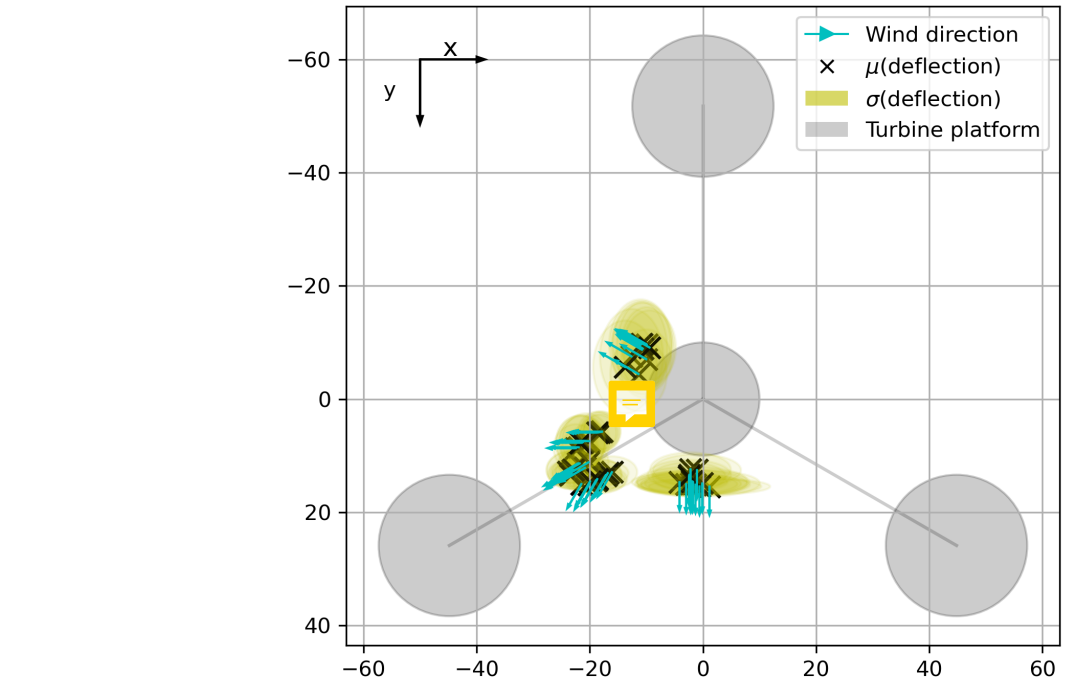

Figure 11. Mean and standard deviation of the floater position shown in context of the floater geometry.

with the initial screening of the motion envelope of the floater in figure 9 larger displacements are observed when wind, waves and current directions are aligned. This is not surprising considering the magnitude of the current and the size and shape of the floater. Although the wind forcing is the largest contributor to the main platform motions, the direction and magnitude of the waves and current will cause significant variations around main direction of displacement, as can be observed in figure 12. These variations are expected to impact both fatigue and extreme loads, and indicate that the importance of running a much larger set of load cases in which all variations of both magnitude and direction of wind, waves, and current.

6 Conclusions

In this publication a proof-of-concept is presented to perform a first step in either a design adjustment study or a site suitability assessment of a floating wind turbine and its dynamic power cable.

The results give an overview of some of the analysis steps needed to assess the dynamic loading conditions of a dynamic power cable transporting power to and from a floating wind turbine in a wind farm (to and from refer to the next and previous turbine in the power cable array). One of those steps is the modelling of the dynamic power cable since its bending stiffness drives to a large extend the response. The authors show that adding bending stiffness to a catanary mooring line element

https://doi.org/10.5194/wes-2024-24
Preprint. Discussion started: 29 April 2024

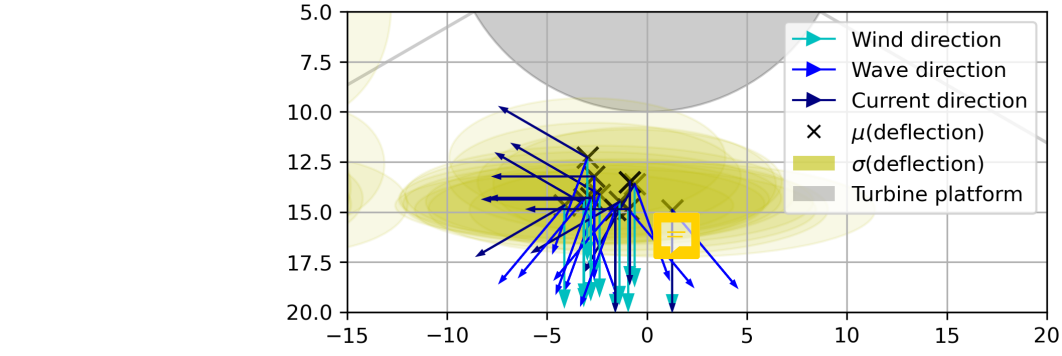

Figure 12. Close up of an overview of simulations with wind direction of 0°.

(implemented in HAWC2 and ESYSMooring) can match the static response obtained from a well established industrial tool such as DeepLines (see section 3).

With respect to the design of the lazy wave the results of the parametric design performed by Rentschler et al. (2019) is re-used for this work. In the dynamic simulation environment HAWC2 a few steps are needed to calculate a robust steady state starting point, and a geometrical shape that is sufficiently similar to the lazy wave is shown to work well for that purpose in section 4.3.

The IEA15MW reference turbine in combination with the UMaine semi-sub floater design have been used as a case study considering a site at an undisclosed location and using met-ocean data from a measurement campaign. In an industrial context an extensive design analysis would be required to adjust the mooring lines, turbine controller tuning, dynamic power cable bend-stiffener connection with the floater, and potentially the floater dimensions and tower to assure the system operates within its limits at the given site. For this study the mooring lines have been simply scaled back to account for the change in water depth from 200 to 82 meter, and the portion resting on the ocean floor has been extended to avoid stretching the line (and directly loading the anchors) considering the initial screening conditions defined in table 5. Note that the turbine controller tuning, tower and floater geometry have not been changed with respect to the reference definition in Allen et al. (2020). The connection between the dynamic power cable and the floating platform was simplified as a ball bearing joined. A sanity check by means of a decay test of the floater confirms that the system eigenfrequencies (of the combined floater-turbine-mooring lines) remain very close the reference reported in Allen et al. (2020).

To evaluate the preliminary design concept for this specific site, a reduced set of load cases is defined (section 5.3): one centered around wave conditions with a return period of 50 years, rated wind speed, and in which wind and waves are aligned (see table 5). A more extensive set cases is described in section 5.4 (now including water current) to cover normal operating conditions (see table 6). It is noted that the initial screening conditions from table 5 are smaller when compared to the response using smaller waves but now with water current.

Finally it is concluded that with the steps outlined in this proof of concept one can perform a detailed and extensive analysis of the fitness of a dynamic power cable, mooring lines, turbine and floater response.

https://doi.org/10.5194/wes-2024-24
Preprint. Discussion started: 29 April 2024

eawe european academy of wind energy
Open Access WIND ENERGY SCIENCE DISCUSSIONS

Appendix A: Mooring line with bending stiffness in HAWC2

The implementation of a mooring line element with bending stiffness in this publication is utilising the External System (ESYS) interface of HAWC2. The mooring line element was originally developed by Kallesøe (2011); Hansen and Kallesøe (2011) and the work presented here extends that by also including bending a stiffness component between three connected nodes. By utilising the HAWC2 ESYS interface the formulation and solution of the mooring line element with bending stiffness is highly integrated into the solution procedure of HAWC2 and a brief overview of the latter can be found in chatper 3 of Gözcü (2020).

ESYS provides a mechanism to tightly couple a user defined and programmed extension to HAWC2. There are two main elements that have to be provided: the unconstrained equations of motion of the system, and any constraints between the system and the HAWC2 model. With these inputs, HAWC2 will bring the defined model into the general solution procedure and using a Newmark time integration scheme. For a more detailed description of the general solution procedure the reader is referred to chapter 3 of Gözcü (2020)). The scope of this publication is to indicate what elements the model of the mooring line with bending stiffness are provided into the HAWC2 solution scheme via the general External Systems (ESYS) interface.

The HAWC2 interface will provide the generalized coordinates and its derivatives (the q's in equation A1), and requires the ESYS model to set the equivalent mass, stiffness and damping matrices of the equations of motion. Additionally, the residual of the dynamical system and the relevant constraints have to be computed. In general terms this means an ESYS model implementation should provide:

$$r_q = M\ddot{q} + C\dot{q} + Kq - f_{ext} + G\lambda \tag{A1}$$

where q refers to the nodal states (having six degrees of freedom) and its derivatives (locations, velocity, accelerations), M, C, K the system mass, damping and stiffness matrices respectively, f the external forces (such as buoyancy and hydrodynamic drag) and $G\lambda$ the constraint forces. This happens in the following order:

1. Compute ESYS system matrices M, C, K. For a dynamical system these usually are a function of the generalised coordinates q, step 4 in section 3.1.5 of Gözcü (2020).
2. Compute external forces on the cable (hydrodynamic drag, buoyancy): f_{ext} in equation A1.
3. Update constraints, step 4 in section 3.1.5 of Gözcü (2020).
4. Calculate residuals (equation A1, step 5 in section 3.1.5 of Gözcü (2020)).

Note that the above is only part of the more elaborate HAWC2 solution scheme at each time step.

The basis for the cable element is, as describe in Hansen and Kallesøe (2011), based on a similar approach as outlined in Bergan et al. (1985). The axial force in the cable is defined by the Green strain:

$$\epsilon_G = \frac{L_n^2 - L_{n,0}^2}{2L_{n,0}^2} \tag{A2}$$

https://doi.org/10.5194/wes-2024-24
Preprint. Discussion started: 29 April 2024

eawe european academy of wind energy
Open Access WIND ENERGY SCIENCE DISCUSSIONS

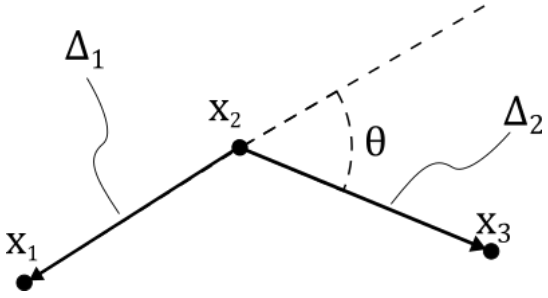

Figure A1. Definition of the angle θ between three connecting nodes.

where L_n refers to the length under loading, and $L_{n,0}$ to the unloaded state. The corresponding axial force in a cable element is then:

$$f = EA\epsilon_G \tag{A3}$$

where E is the Young's modulus and A the cross sectional area.

The bending stiffness in the cable is simply driven by the angle θ between three nodes (as shown in figure):

$$M = \frac{EI}{L_n}\theta \tag{A4}$$

and where M refers to the resulting bending moment due the curvature θ and given bending stiffness and element length EI, L_n respectively.

Author contributions. David Verelst adjusted and prepared the HAWC2 model of the turbine, floater, mooring lines and dynamic cable (including initialisation and verification with DeepLines) for the site specific study of this publication. Jean-Philippe Roques provided the DeepLines analysis. Rasmus Lund performed the verification between the HAWC2 Timoshenko beam element, ESYSMooring and the analytical Bernoulli-Euler solution. Rasmus executed and analysed the response analysis of the system under various met-ocean conditions. All three authors reviewed and commented on the publication text and figures.

Competing interests. The presented work shows results of the hydro-servo-aeroelastic framework HAWC2 that is developed by DTU Wind (the first and second author's employer). HAWC2 is available free of charge for academic use, but is also made available under commercial terms for industrial parties. This work was funded by TotalEnergies and is the employer of the third listed author. Both are clearly indicated in the competing interests and Acknowledgement sections of the publication.

https://doi.org/10.5194/wes-2024-24
Preprint. Discussion started: 29 April 2024

260 *Acknowledgements.* This work was supported by TotalEnergies OneTech under the Anticipation & Portfolio Performance Incubation program. Authors would like to thank Lars Oberbeck from TotalEnergies for the support and input along the execution of this project. Further, the authors are grateful for the support in scoping, guiding and reviewing the project from DTU's side by Katherine Dykes and Henrik Bredmose. Finally, the authors would like to thank Anders Melchior Hansen for deriving and implementing the cable element with bending stiffness into the HAWC2-ESYSMooring modelling framework.

https://doi.org/10.5194/wes-2024-24
Preprint. Discussion started: 29 April 2024

eawe european academy of wind energy
Open Access WIND ENERGY SCIENCE DISCUSSIONS

References

Allen, C., Viselli, A., Dagher, H., Goupee, A., Gaertner, E., Abbas, N., Hall, M., and Barter, G.: Reference turbine (semisubmersible variant) description report, Report, NREL, Golden, CO, United States, https://www.nrel.gov/docs/fy20osti/76773.pdf, 2020.

Bergan, P. G., Mollestad, E., and Sandsmark, N.: Non-linear static and dynamic response analysis for floating offshore structures, Engineering Computations, 2, 13–20, https://doi.org/10.1108/eb023596, publisher: MCB UP Ltd, 1985.

Gaertner, E., Rinker, J., Latha, S., Zahle, F., Anderson, B., Barter, G., Abbas, N., Meng, F., Bortolotti, P., Skrzypinski, W., Scott, G., Feil, R., Bredmose, H., Dykes, K., Shields, M., Allen, C., and Viselli, A.: Definition of the IEA 15-Megawatt Offshore Reference Wind Turbine, Report, NREL, Golden, CO, United States, https://www.nrel.gov/docs/fy20osti/75698.pdf, 2020.

Gözcü, M. O.: Wind turbine blade large deflections: A non-intrusive method for blade nonlinear reduced order models, PhD, DTU Wind Energy, https://dx.doi.org/10.11581/dtu:00000082, publisher: DTU Wind Energy, 2020.

Gözcü, O. and Verelst, D. R.: The effects of blade structural model fidelity on wind turbine load analysis and computation time, Wind Energy Science, 5, 503–517, https://doi.org/10.5194/wes-5-503-2020, publisher: Copernicus GmbH, 2020.

Hansen, A. M.: Implementation of HAWC2 interface to WAMIT, Tech. Rep. DTU Wind Energy Report-I-0236, DTU Wind Energy, 2014.

Hansen, A. M. and Kallesøe, B. S.: Detailed and reduced models of dynamic mooring system, Tech. Rep. Risø-R-1803(EN), https://orbit.dtu.dk/en/publications/detailed-and-reduced-models-of-dynamic-mooring-system, 2011.

Kallesøe, B. S.: Nonlinear beam element in HAWC2 for modeling of mooring systems, Tech. Rep. Risø-R-1769(EN), https://orbit.dtu.dk/en/publications/nonlinear-beam-element-in-hawc2-for-modeling-of-mooring-systems, 2011.

Kim, T., Hansen, A. M., and Branner, K.: Development of an anisotropic beam finite element for composite wind turbine blades in multibody system, Renewable Energy, 59, 172–183, https://doi.org/10.1016/j.renene.2013.03.033, 2013.

Larsen, T. J. and Hansen, A. M.: How 2 HAWC2, the user's manual, Tech. rep., DTU Wind Energy, 2023.

Lund, R. S. and Verelst, D. R.: Dynamic Modelling and Response of a Power Cable connected to a Floating Wind Turbine, https://doi.org/10.11583/DTU.25577157, 2024.

Madsen, H. A., Larsen, T. J., Pirrung, G. R., Li, A., and Zahle, F.: Implementation of the blade element momentum model on a polar grid and its aeroelastic load impact, Wind Energy Science, 5, 1–27, https://doi.org/10.5194/wes-5-1-2020, 2020.

Pavese, C., Wang, Q., Kim, T., Jonkman, J. M., and Sprague, M. A.: HAWC2 and BeamDyn: Comparison Between Beam Structural Models for Aero-Servo-Elastic Frameworks, in: Proceedings of the EWEA Annual Event and Exhibition 2015, Paris, France, http://orbit.dtu.dk/files/118348455/HAWC2_and_BeamDyn_paper.pdf, 2015.

Rentschler, M. U. T., Adam, F., and Chainho, P.: Design optimization of dynamic inter-array cable systems for floating offshore wind turbines, Renewable and Sustainable Energy Reviews, 111, 622–635, https://doi.org/10.1016/j.rser.2019.05.024, 2019.

Thies, P. R., Johanning, L., and Smith, G. H.: Assessing mechanical loading regimes and fatigue life of marine power cables in marine energy applications, Proceedings of the Institution of Mechanical Engineers, Part O: Journal of Risk and Reliability, 226, 18–32, https://doi.org/10.1177/1748006X11413533, 2012.